

2024

Lung-Delivered IL-10 Therapy Elicits Beneficial Effects via Immune Modulation in Organic Dust Exposure-Induced Lung Inflammation

Aaron D. Schwab

Todd A. Wyatt

Amy J. Nelson

Angela Gleason

Rohit Gaurav

See next page for additional authors

Tell us how you used this information in this [short survey](#).

Follow this and additional works at: https://digitalcommons.unmc.edu/com_pulm_articles



Part of the [Allergy and Immunology Commons](#), [Critical Care Commons](#), [Respiratory System Commons](#), and the [Respiratory Tract Diseases Commons](#)

Authors

Aaron D. Schwab, Todd A. Wyatt, Amy J. Nelson, Angela Gleason, Rohit Gaurav, Debra J. Romberger, and Jill A. Poole



Lung-delivered IL-10 therapy elicits beneficial effects via immune modulation in organic dust exposure-induced lung inflammation

Aaron D. Schwab, Todd A. Wyatt, Amy J. Nelson, Angela Gleason, Rohit Gaurav, Debra J. Romberger & Jill A. Poole

To cite this article: Aaron D. Schwab, Todd A. Wyatt, Amy J. Nelson, Angela Gleason, Rohit Gaurav, Debra J. Romberger & Jill A. Poole (2024) Lung-delivered IL-10 therapy elicits beneficial effects via immune modulation in organic dust exposure-induced lung inflammation, Journal of Immunotoxicology, 21:1, 2332172, DOI: [10.1080/1547691X.2024.2332172](https://doi.org/10.1080/1547691X.2024.2332172)

To link to this article: <https://doi.org/10.1080/1547691X.2024.2332172>



© 2024 The Author(s). Published by Informa UK Limited, trading as Taylor & Francis Group.



[View supplementary material](#)



Published online: 02 Apr 2024.



[Submit your article to this journal](#)



Article views: 169

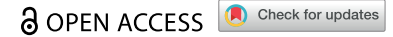


[View related articles](#)



[View Crossmark data](#)

RESEARCH ARTICLE



Lung-delivered IL-10 therapy elicits beneficial effects via immune modulation in organic dust exposure-induced lung inflammation

Aaron D. Schwab^a, Todd A. Wyatt^{b,c,d}, Amy J. Nelson^a, Angela Gleason^a, Rohit Gaurav^a, Debra J. Romberger^{b,c} and Jill A. Poole^a

^aDivision of Allergy and Immunology, Department of Internal Medicine, College of Medicine, University of Nebraska Medical Center, Omaha, NE, USA; ^bResearch Service, Veterans Affairs Nebraska-Western Iowa Health Care System, Omaha, NE, USA; ^cDivision of Pulmonary, Critical Care & Sleep, Department of Internal Medicine, College of Medicine, University of Nebraska Medical Center, Omaha, NE, USA; ^dDepartment of Environmental, Agricultural and Occupational Health, College of Public Health, University of Nebraska Medical Center, Omaha, NE, USA

ABSTRACT

Efficacious therapeutic options capable of resolving inflammatory lung disease associated with environmental and occupational exposures are lacking. This study sought to determine the preclinical therapeutic potential of lung-delivered recombinant interleukin (IL)-10 therapy following acute organic dust exposure in mice. Here, C57BL/6J mice were intratracheally instilled with swine confinement organic dust extract (ODE) (12.5%, 25%, 50% concentrations) with IL-10 (1 µg) treatment or vehicle control intratracheally-administered three times: 5 hr post-exposure and then daily for 2 days. The results showed that IL-10 treatment reduced ODE (25%)-induced weight loss by 66% and 46% at Day 1 and Day 2 post-exposure, respectively. IL-10 treatment reduced ODE (25%, 50%)-induced lung levels of TNF α (–76%, –83% [reduction], respectively), neutrophil chemoattractant CXCL1 (–51%, –60%), and lavage fluid IL-6 (–84%, –89%). IL-10 treatment reduced ODE (25%, 50%)-induced lung neutrophils (–49%, –70%) and recruited CD11c^{int}CD11b⁺ monocyte-macrophages (–49%, –70%). IL-10 therapy reduced ODE-associated expression of antigen presentation (MHC Class II, CD80, CD86) and inflammatory (Ly6C) markers and increased anti-inflammatory CD206 expression on CD11c^{int}CD11b⁺ cells. ODE (12.5%, 25%)-induced lung pathology was also reduced with IL-10 therapy. In conclusion, the studies here showed that short-term, lung-delivered IL-10 treatment induced a beneficial response in reducing inflammatory consequences (that were also associated with striking reduction in recruited monocyte-macrophages) following acute complex organic dust exposure.

ARTICLE HISTORY

Received 3 January 2024
Revised 11 March 2024
Accepted 14 March 2024

KEYWORDS

Organic dust; therapy; immunology; inflammation; lung disease


Introduction

Chronic respiratory diseases including chronic obstructive pulmonary disease, asthma, hypersensitivity pneumonitis, pulmonary fibrosis, and chronic bronchitis have been associated with inhalant exposure to materials commonplace in production agriculture (Agustí et al. 2012; Nordgren and Bailey 2016; Wunschel and Poole 2016; Park et al. 2021). Though long-term low-level exposures are associated with disease manifestations, a one-time high-dose inhalant exposure to a biohazard can cause lung injury and inflammation and potentially lead to irreversible disease. A striking example of this phenomenon is organic dust toxic syndrome (ODTS), a noninfectious febrile illness that occurs 4–12 hr following a single concentrated organic dust exposure, often one high in endotoxin or lipopolysaccharide (LPS) content (Madsen et al. 2012). Inhalant exposure to organic dusts derived from animal confinement facilities, grain, animal feed, and hay increases the odds of developing an adverse respiratory disease (Sigsgaard et al. 2020). These agricultural dusts are complex and heterogeneous collections of various particulate matter and particle-related bacterial, archaeobacterial, and fungal components

that cause inflammatory reactions in the lungs (Boissy et al. 2014).

Despite modernization of facilities, improvements in outreach efforts, and amplified awareness of occupational hazards and exposure prevention, respiratory disease remains a significant healthcare burden for exposed workers (May et al. 2012; Poole 2012; Basinas et al. 2015). Given efficacious therapeutic options for exposed workers are lacking, targeted therapeutic interventions capable of ameliorating lung inflammation post-exposure and preventing progression toward a chronic disease state are of importance. Exploiting the anti-inflammatory interleukin (IL)-10 cytokine pathway is a potential therapeutic strategy for these occupational bioaerosol-exposed persons. In veterans with farming experience, blood baseline IL-10 concentrations were inversely associated with pro-inflammatory cytokine release after adjusting for potential confounders (LeVan et al. 2018). In a murine model of repetitive swine confinement facility organic dust extract (ODE) exposure-induced lung inflammation, IL-10-deficient animals exhibited potentiated inflammatory lung histopathology and neutrophil influx with reversal by recombinant IL-10 treatment (Wyatt et al. 2020). Moreover, lung-delivered IL-10

CONTACT Aaron D. Schwab  aaron.schwab@unmc.edu  Division of Allergy and Immunology, Nebraska Medical Center, Omaha, NE 68198, USA.

 Supplemental data for this article can be accessed online at <https://doi.org/10.1080/1547691X.2024.2332172>.

© 2024 The Author(s). Published by Informa UK Limited, trading as Taylor & Francis Group.

This is an Open Access article distributed under the terms of the Creative Commons Attribution License (<http://creativecommons.org/licenses/by/4.0/>), which permits unrestricted use, distribution, and reproduction in any medium, provided the original work is properly cited. The terms on which this article has been published allow the posting of the Accepted Manuscript in a repository by the author(s) or with their consent.

treatment following acute LPS exposure reduced LPS-induced influx of lung neutrophils, lymphocyte sub-populations, and histopathology, as well as reduced the recruitment of a transitional monocyte-macrophage sub-population (Poole et al. 2022). This latter observation may be critical as a growing body of evidence supports a significant role for sub-populations of recruited, often inflammatory and pro-fibrotic, monocytes/macrophages in chronic lung diseases (Misharin et al. 2017; Hu and Christman 2019). Strategies to target and potentially reduce these infiltrating cells are needed. However, it is not known whether lung-targeted IL-10 therapy could reduce adverse respiratory health consequences following exposure to complex organic dust exposure(s).

The hypothesis of this preclinical murine study was that treatment with lung-delivered IL-10 would reduce the inflammatory consequences following a one-time ODE exposure in mice. The objective of this study was to determine the effect of short-term IL-10 treatment with the airway inflammatory characteristics of ODE-induced disease as well as characterize the immune phenotype and function of the associated infiltrating lung monocyte-macrophage sub-populations in an animal model to reduce lung disease burden in exposed workers.

Materials and methods

Animal exposure model

C57BL/6 mice (between 6 and 8 wk-of-age) were purchased from The Jackson Laboratory (Bar Harbor, ME), randomized upon arrival, and allowed to acclimate for 1 wk prior to initiation of experiments (Note: Authors A.J.N., A.G., and facility staff were aware of the randomization, whereas all other authors were blinded). Male mice were utilized for all studies because we have previously demonstrated that female mice were less susceptible to inflammatory agent inhalation-induced airway and systemic inflammatory effects (Nelson et al. 2018). Airway inflammation was induced using intratracheal instillation of a previously-characterized organic dust extract (ODE) (Boissy et al. 2014) whereby mice were lightly sedated under isoflurane (VetOne, Boise, ID) and received treatment with either 50 μ l of sterile saline or ODE (12.5, 25, or 50% to assess concentration-dependent effects). An intubation laryngoscope (Harvard Apparatus, Holliston, MA) enabled tracheal visualization and access for the intratracheal instillation technique. IL-10 was purchased from R&D Systems (Minneapolis, MN) and intratracheally administered at 1 μ g in 50 μ l of sterile saline vs. vehicle control (sterile saline) as previously reported (Poole et al. 2022). Weights were recorded throughout the treatment period. For euthanization, mice were sedated and euthanized with isoflurane, followed by exsanguination (right axillary blood collection).

Organic dust extract

An aqueous solution of ODE was prepared from swine confinement feeding facilities as previously described (Poole et al. 2019). In brief, settled surface dust (1 g) was incubated in sterile Hank's Balanced Salt Solution (10 ml; Mediatech, Manassas, VA) for 1 hr and centrifuged twice for 30 min at 2850 \times g; the final supernatant was then filter-sterilized (0.22 μ m) to remove microorganisms and coarse particles. Stock ODE was batch prepared and stored at -20°C ; aliquots were diluted for each experiment to a final concentration (vol/vol) of 12.5, 25, or 50% in sterile phosphate buffered saline (PBS, pH 7.4; diluent). Endotoxin concentrations were determined using a limulus amoebocyte lysate assay

(Lonza, Walkersville, MD). Endotoxin levels averaged 2.616–5.232 μ g (\sim 25–100 EU) for 50% ODE, 1.308–2.616 μ g (\sim 10–50 EU) for 25% ODE, and 0.654–1.308 μ g (\sim 6–25 EU) for 12.5% ODE by limulus amoebocyte assay. Whereas 12.5% ODE has been shown to be well-tolerated in repetitive exposure modeling, the optimal ODE concentration for acute exposure modeling has not been previously investigated (Poole et al. 2009, 2019).

Blood collection and serum

Whole blood was collected from the axillary artery at euthanasia and serum harvested as described in Poole et al. (2019). Serum pentraxin-2 (murine acute phase reactant protein) levels were assessed using a Quantikine ELISA kit (R&D, Minneapolis, MN), according to manufacturer instructions (minimal detection difference [MDD] of 0.159 ng/ml).

Inflammatory marker analysis

Bronchoalveolar lavage fluid (BALF) was collected from each host using three sequential 1-ml injections/recoveries with sterile phosphate buffered saline (PBS, pH 7.4). Each isolate was first centrifuged (with supernatant of first lavage fraction being saved for cytokine/chemokine analyses), and then total cell numbers from the combined recovered cell pellets were enumerated using a BioRad TC 20 cell counter; aliquots of the isolated cells were then used to perform differential cell counts from cytopsin-prepared slides (Cytopro Cyto centrifuge, ELITech Group, Logan, UT) that had been stained with Diff-Quick (Siemens, Newark, DE). After BALF isolation, lung tissue homogenates were prepared by homogenizing lung samples (1/2 of each right lung) in 500 μ l sterile PBS. Levels of tumor necrosis factor (TNF)- α , IL-6, IL-10, and murine neutrophil chemokines (CXCL1 and CXCL2) in the first lavage cell-free supernatant and the lung tissue homogenates were then quantitated by ELISA (R&D Systems) following manufacturer instructions. The kits had MDD of 1.88, 1.6, 31.3, 2.0, and 1.5 pg/ml for TNF α , IL-6, IL-10, CXCL1, and CXCL2, respectively.

Lung cell staining and flow cytometry

Following removal of blood from the pulmonary vasculature and after BALF removal, harvested lungs (remaining 1/2 of each right lung) were subjected to an automated dissociation procedure using a gentleMACS Dissociator instrument (Miltenyi Biotech, Auburn, CA) (Poole et al. 2019). Lung cells from each animal were enumerated and then incubated with a LIVE/DEAD Fixable Blue Dead Cell Stain Kit (Invitrogen, Carlsbad, CA) and CD16/32 (Fc Block, BioLegend, San Diego, CA) to minimize non-specific antibody staining. For immune cell characterization, dedicated aliquots of the cells were then stained with fluorophore-conjugated monoclonal antibody against rat anti-mouse CD45 (clone: 30-F11; BD Biosciences, Franklin Lake, NJ), CD11b (clone: M1/70; BD Biosciences), Ly6G (clone: 1A8; BD Biosciences), CD11c (clone: N418; Invitrogen), CD4 (clone: RM4-5; BD Biosciences), CD8 (clone: 53-6.7; BD Biosciences), CD19 (clone: 1D3; Invitrogen), hamster anti-mouse CD3e (clone: 145-2C11; BD Biosciences), or mouse anti-mouse NK1.1 (clone: PK136; BD Biosciences). Cells were then acquired on a BD LSRII Yellow/Green cytometer. In each case, a minimum of 50,000 events were acquired and analyzed for each sample.

Post-acquisition, all flow cytometry data were exported and stored using the flow cytometry standard (FCS) 3.1 format and subsequently analyzed using FlowJo software version 10.8 (FlowJo, Ashland, OR). The gating strategies for Ly6G⁺ neutrophils, CD11c⁺CD11b^{lo} alveolar (Alv) macrophages (M ϕ), CD11c⁺CD11b⁺ activated (Act) M ϕ , CD11c^{int}CD11b⁺ recruited/transitioning monocytes-M ϕ , and CD11c⁻CD11b⁺ monocytes, CD3⁺CD4⁺ T-cells, CD3⁺CD8⁺ T-cells, CD19⁺ B-cells, and NK cells were performed as previously reported (Poole et al. 2012, 2017, 2022; Robbe et al. 2015; Nelson et al. 2018; Mikuls et al. 2021). The percentage of all respective cell populations was determined from live CD45⁺ lung leukocytes after excluding debris and doublets. This percentage was multiplied by the respective total lung cell numbers to determine specific cell population numbers for each animal.

To further characterize immuno-phenotypes of the four monocyte-macrophage sub-populations, additional dedicated aliquots of the cells were stained with fluorophore-conjugated monoclonal antibody against Ly6C (clone: HK1.4; BioLegend), F4/80 (clone: T45-2342; BD Biosciences), MHC Class II (I-A/I-E) (clone: M5/114.15.2; Cell Signaling Technology), CD86 (clone: GL-1; BioLegend), CD206 (clone: C068C2; BioLegend), IL-10 (clone: JES5-16E3; BioLegend), TNF α (clone: MP6-XT22; BioLegend), or CD80 (clone: 16-10A1; BD Biosciences). The cells were then analyzed as outlined above.

Lung myeloid cell functional assays

In separate studies, phagocytic ability and reactive oxygen species (ROS) production were determined for lung monocytes/macrophages isolated from whole lungs of additional sets of exposed mice (not lavaged as in studies above). Specifically, at 48 hr post-exposure, lung cell suspensions were prepared and then aliquots of cells (3.0×10^5 /sample) were incubated for 30 min at 37°C with 25 μ M CellRox Deep Red (Invitrogen) or with opsonized fluorescein-conjugated *Escherichia coli* BioParticles (Invitrogen) at a 20 particles/cell ratio to quantify ROS and phagocytic activity, respectively, per manufacturer instructions. These same cells were then placed on ice and incubated as described above for markers indicative of monocytes-macrophages and neutrophils (i.e. live/dead, CD45, CD11b, CD11c, Ly6C, Ly6G). Cells were subsequently washed with cold PBS, fixed with 4% paraformaldehyde, and then evaluated on that same day in the BD LSRII YG (Green Profile) system.

Lung histopathology

Post-lavage, each left lung was excised and inflated to 15 cm H₂O pressure with 10% formalin (Fisher Scientific, Fair Lawn, NJ) for 24 hr to preserve pulmonary architecture as described in Poole et al. (2019). The fixed lobes were then placed into cassettes, embedded in paraffin, cut (to 4–5 μ m) at midpoint sections to include regions of both large and small airways as well as blood vessels, and stained with hematoxylin and eosin (H&E). Slides were then reviewed at all scanning magnifications by an experimental pathologist blinded to the treatment conditions and semi-quantitatively assessed for degree and distribution of lung inflammation. Using a previously-published scoring system, each lung was given an inflammatory score value from 0 to 4 (higher score indicating greater inflammatory changes in lung) (Wyatt et al. 2020).

Statistical analysis

Sample-size calculation was estimated from a previous study assessing the effect of IL-10 treatment post-endotoxin exposure in C57BL/6 male mice (Poole et al. 2022) whereby a sample size of $n=4$ was calculated in each group to achieve 80% power at a 0.05 level of significance—to detect a difference in TNF α (pg/ml), assuming a mean (SD) of 128 (30) for the vehicle group and a mean (SD) of 20 (30) for the IL-10 treatment group, both post-endotoxin exposure. Experimental groups included at least four mice/group. For the various ODE concentrations used in these acute exposure modeling studies (with or without IL-10 treatment), the maximum possible number of mice/group was $n=4$ for the saline control group, $n=5$ for the 12.5% ODE + vehicle, $n=5$ for the 12.5% ODE + IL-10, $n=7$ for the 25% ODE + vehicle, $n=9$ for the 25% ODE + IL-10, $n=5$ for the 50% ODE + vehicle, and $n=5$ for the 50% ODE + IL-10 group. For immune phenotype and functional studies, the total maximum possible was $n=10$ per group. Numbers less than the maximum number reflect limitations in the available sample quantity or quality.

Data are presented as the mean \pm SEM. To detect significant changes among three or more groups, a one-way analysis of variance (ANOVA) was utilized and a *post-hoc* test (Tukey/LSD) was performed to account for multiple comparisons if the p -value was < 0.05 . A Mann-Whitney test was used to detect significant changes between two groups. All statistical analyses were performed using Prism software (v.9.5.1, GraphPad, San Diego, CA). Statistical significance was accepted at a two-sided p -value < 0.05 .

Ethics statement

Neither human participants, data, nor tissues were used in these studies. The study was conducted and reported in accordance with ARRIVE guidelines (<https://arriveguidelines.org>). All animal procedures were approved by the University of Nebraska Medical Center (UNMC) Institutional Animal Care and Use Committee and were in accordance with NIH guidelines for the use of rodents.

Results

Lung-delivered IL-10 therapy reduces weight loss, serum pentraxin levels, and airway inflammatory cell influx following ODE exposure

In these experiments, mice were intratracheally-instilled with ODE at various concentrations (12.5, 25, 50%) followed by three doses of IL-10 or saline vehicle intratracheally instilled at 5, 24, and 48 hr following the single ODE exposure (schematic of experimental design: Figure 1A). The results showed that treatment with IL-10 significantly reduced ODE-induced weight loss at Days 1 and 2 with the 25% ODE ($p < 0.001$) but not with the 12.5 and 50% ODE concentrations (Figure 1B). ODE increased serum levels of the murine acute phase reactant protein pentraxin-2 in a concentration-dependent manner; this response was reduced with IL-10 treatment for the 25 and 50% ODE concentrations (Figure 1C). There was a concentration-dependent increase in total airway cellular influx (marked by neutrophils and to a lesser degree macrophages) following ODE exposure (Figure 1D). Moreover, treatment with IL-10 decreased the influx of total number of BALF cells with all test ODE concentrations (Figure 1D). Neutrophil influx was decreased following IL-10 therapy at 25 and 50% (but not 12.5%) ODE concentrations, and

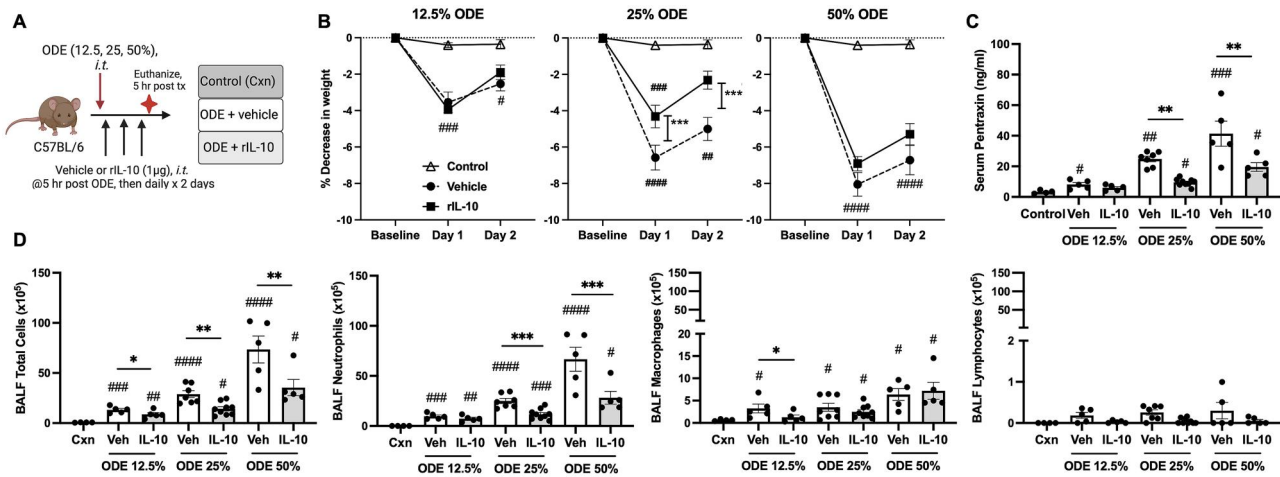


Figure 1. Lung-delivered IL-10 therapy reduces weight loss, serum pentraxin-2 levels, and airway inflammatory cell influx following a one-time ODE exposure. (A) Experimental design schematic (created with BioRender.com). (B) Line graphs depict mean (\pm SEM) weight changes over time with ODE (12.5, 25, 50% concentration)-exposed mice treated with IL-10 vs. vehicle (Veh) vs. control (Cxn, saline treated mice, no ODE). (C) Scatter-dot plots depict mean with SEM bars among treatment groups of serum pentraxin-2 levels. (D) Total cellular influx and leukocyte cell numbers quantitated in bronchoalveolar lavage fluid (BALF). $N = 4$ (Cxn) and $N = 5-9$ (Veh, IL-10) mice/group. Statistical significance vs. Cxn ($^{\#}p < 0.05$, $^{\#\#}p < 0.01$, $^{\#\#\#}p < 0.001$, $^{\#\#\#\#}p < 0.0001$); between groups ($^*p < 0.05$, $^{**}p < 0.01$, $^{***}p < 0.001$).

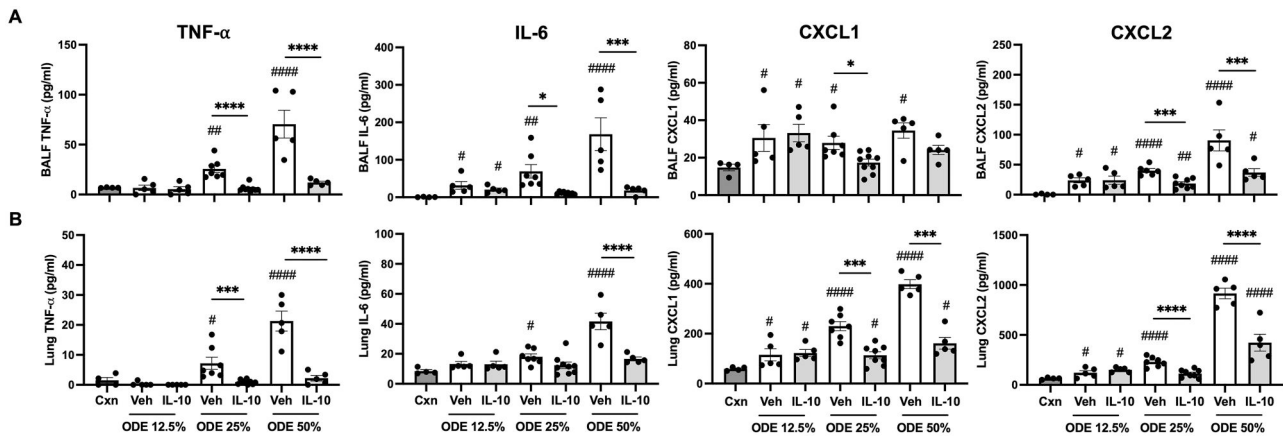


Figure 2. Lung-delivered IL-10 therapy reduces inflammatory cytokines/chemokines following a one-time ODE exposure. Levels of airway inflammatory markers determined by ELISA from (A) BALF and (B) lung homogenates. $N = 4$ (Cxn) and $N = 5-9$ (Veh, IL-10) mice/group. Statistical significance vs. Cxn ($^{\#}p < 0.05$, $^{\#\#}p < 0.01$, $^{\#\#\#}p < 0.0001$); between groups ($^*p < 0.05$, $^{**}p < 0.01$, $^{***}p < 0.001$, $^{****}p < 0.0001$).

BALF macrophages were reduced by IL-10 treatment for the 12.5%—but not the 25 and 50%, ODE concentrations. BALF lymphocyte levels were not significantly induced by ODE treatments. Eosinophils were rare and did not differ among treatment groups (data not shown).

Lung-delivered IL-10 treatment reduces ODE-induced inflammatory analytes

In these mice, BALF and lung homogenates were examined for inflammatory markers consistent with airway inflammatory processes associated with agriculture-induced lung disease (American Thoracic Society 1998). At 48 hr post-ODE exposure, BALF levels of IL-6 and the murine chemoattractants (CXCL1 and CXCL2) were increased with all ODE concentrations; in comparison, levels of TNF α were elevated with 25 and 50%, but not 12.5%, ODE (Figure 2A). Levels of these airway inflammatory markers (TNF α , IL-6, CXCL1, CXCL2) were all reduced with IL-10 treatment for the 25% and 50% ODE exposures, with the exception that CXCL1 was only reduced with IL-10 treatment in the case of 25% ODE (Figure 2A). IL-10 treatment did not significantly alter BALF levels of these

inflammatory cytokines/chemokines with hosts exposed to 12.5% ODE.

Lung homogenates exhibited a similar pattern in that levels of IL-6, CXCL1, and CXCL2 were increased in response to all ODE concentrations, while TNF α levels were increased with 25 and 50% (but not 12.5%) ODE (Figure 2B). Furthermore, IL-10 treatment profoundly reduced 25% and 50% ODE-induced lung homogenate TNF α as well as reduced 50% ODE-induced IL-6 and 25 and 50% ODE-induced CXCL1 and CXCL2 levels (Figure 2B). As expected in response to administration of IL-10, IL-10 levels were increased in both BALF and lung homogenates regardless of ODE concentration levels used in the exposures (Supplemental Figure 1).

Lung-delivered IL-10 treatment reduces ODE-induced lung neutrophil and recruited CD11c^{int}CD11b⁺ monocyte-macrophage cell lung infiltrates

ODE exposure (at all concentrations) increased total lung cell infiltrates; this response was reduced by IL-10 treatment in mice exposed to 50% but not 12.5 or 25% ODE (Figure 3A). ODE-induced lung neutrophil infiltrates (defined as CD11c⁺Ly6G⁺) (Figure 3B) were increased with all ODE concentration exposures, and this response

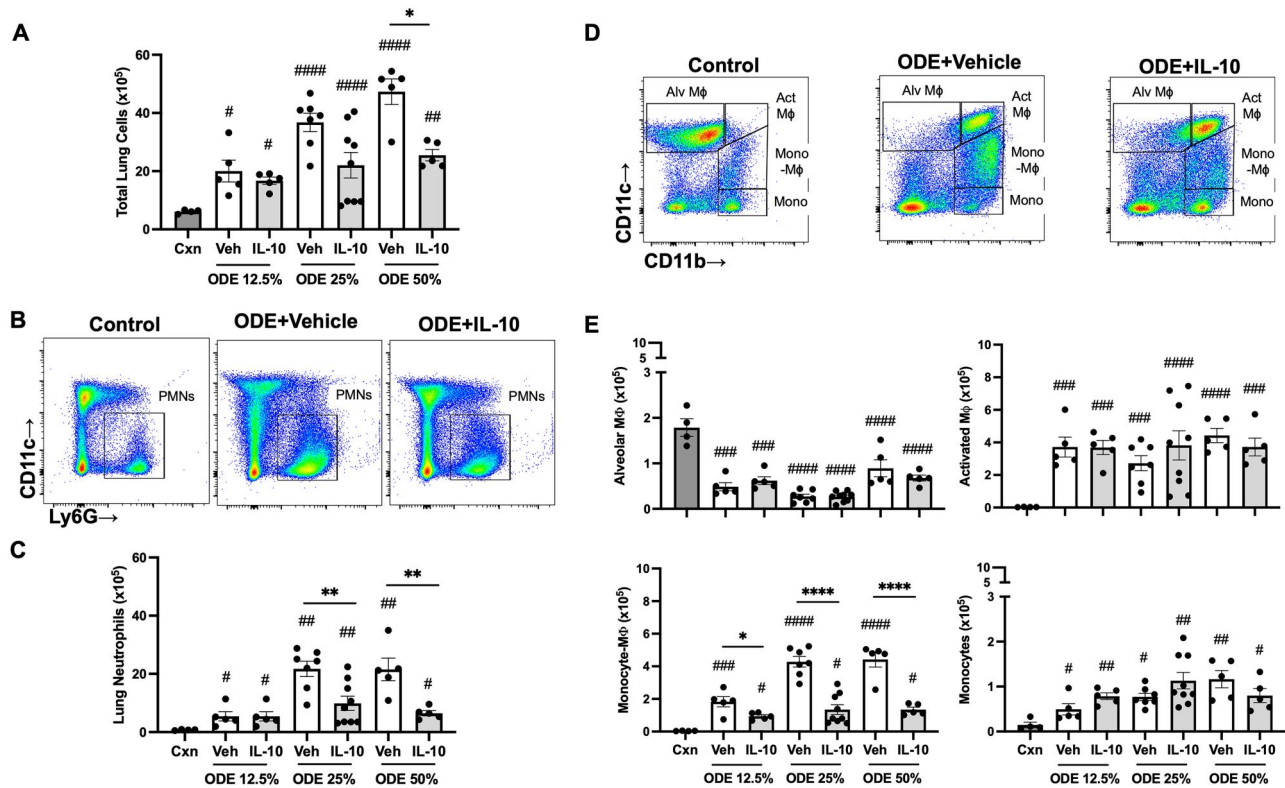


Figure 3. Lung-delivered IL-10 therapy following a one-time ODE exposure modulates total lung and myeloid cell infiltrates. (A) Scatter-dot plots depict mean (\pm SEM) total lung cells across treatment groups of control, ODE + vehicle, and ODE + IL-10 treatment. (B) Representative gate images for lung neutrophils in treatment groups after exclusion of debris, doublets, dead cells, and CD45⁻ cells (with numbers of lung neutrophils [PMN; mean \pm SEM] depicted in scatter-dot plots [C]). (D) Representative gate images for lung macrophage/monocyte Sub-populations in treatment groups: Alveolar macrophages (Alv M Φ) CD11c⁺CD11b^{lo}, Activated macrophages (Act M Φ) CD11c⁺CD11b⁺; Transitioning monocyte/macrophages (Mono-M Φ) CD11c^{int}CD11b⁺; Monocytes (Mono) CD11c⁻CD11b⁺ after exclusion of debris, doublets, dead cells, CD45⁻ cells, and neutrophils [numbers of Sub-populations depicted by scatter-dot plots] (E). Cell numbers determined by multiplying percentage of population from live CD45⁺ cells by total lung cells enumerated. $N=4$ (Cxn) and $N=5-9$ (vehicle, IL-10) mice/group. Statistical significance vs. Cxn ($\#p < 0.05$, $\#\#p < 0.01$, $\#\#\#p < 0.001$, $\#\#\#\#p < 0.0001$); between groups ($*p < 0.05$, $**p < 0.01$, $****p < 0.0001$).

was reduced by IL-10 treatment of hosts exposed to 25 and 50% ODE (Figure 3C). Repetitive ODE exposure is also known to increase CD11c⁺CD11b⁺ activated (Act) macrophage (M Φ) levels and induce recruited/transitioning CD11c^{int}CD11b⁺ monocyte-M Φ infiltrates (Warren et al. 2017). In the current studies, a single ODE exposure increased CD11c⁺CD11b⁺ Act M Φ , CD11c^{int}CD11b⁺ monocyte-M Φ , and CD11c⁻CD11b⁺ monocyte levels—with corresponding decreases in numbers of alveolar (Alv) CD11c⁺CD11b⁺ M Φ (Figure 3D and E) in the lungs of the mice. Strikingly, there was a marked reduction in recruited/transitioning CD11c^{int}CD11b⁺ monocyte-M Φ sub-populations with IL-10 treatment following exposure to any of the ODE concentrations (Figure 3E). IL-10 treatment did not affect levels of Alv M Φ , Act M Φ , or monocyte infiltrates following ODE exposure. Lung CD3⁺CD4⁺ and CD3⁺CD8⁺ T-cell and CD19⁺ B-cell infiltrates were increased by all ODE concentrations in the absence of IL-10; NK cells were increased with only the 50% ODE (Supplemental Figure 2). There were reductions in CD3⁺CD8⁺ T-cell populations due to IL-10 treatment of hosts exposed to 25 or 50% ODE (Supplemental Figure 2). Otherwise, ODE-induced lung lymphocyte infiltrates were not reduced by IL-10 treatment.

Lung-delivered IL-10 therapy following ODE exposure modulates the immuno-phenotype of monocyte/macrophage sub-populations

In the next set of studies, the four monocyte (Mono)/M Φ sub-populations (i.e. Alv M Φ , Act M Φ , Mono-M Φ , Mono) associated

with a one-time ODE (25%) vs. saline (Sal) exposure were further assessed for extracellular/intracellular markers of cellular activation and immuno-phenotype (Figure 4A). F4/80, a marker of monocytes and macrophages, was universally-expressed on both Sal and ODE Mono populations, with a high expression demonstrated on Sal Alv M Φ and ODE Mono-M Φ sub-populations. F4/80 surface expression was down-regulated on ODE Act M Φ . CD206, an anti-inflammatory marker (also referred to as a classic 'M2' marker) (Roszer 2015), was highly-expressed on Sal Alv M Φ and nearly absent among all other monocyte/macrophage sub-populations. Ly6C, a monocyte and activation marker (Wang et al. 2018), demonstrated its highest expression on both Sal and ODE monocytes and its lowest expression on the Sal Alv M Φ . Ly6C expression was increased on ODE Act M Φ and ODE Mono-M Φ cells relative to that seen with Sal Alv M Φ , with ODE Mono-M Φ demonstrating increased Ly6C expression vs. ODE Act M Φ (albeit there was decreased expression of Ly6C with ODE Mono-M Φ vs. Sal and ODE Mono sub-populations). MHC Class II expression, important in antigen presentation (Roche and Furuta 2015), was highest on the ODE Act M Φ , but there was no difference in its expression between the Sal Alv M Φ and ODE Mono-M Φ . Whereas MHC Class II expression was lowest on monocytes, there was increased expression on ODE Mono vs. Sal Mono.

CD80 (co-stimulatory molecule) (Yang et al. 2022) was highly-expressed on both Sal Alv M Φ and ODE Act M Φ . The ODE Mono-M Φ sub-population demonstrated increased CD80 expression vs. both the Sal and ODE Mono populations and decreased expression vs. the Sal Alv M Φ and ODE Act M Φ . CD80 expression was increased on ODE Mono vs. Sal Mono. CD86 (co-stimulatory

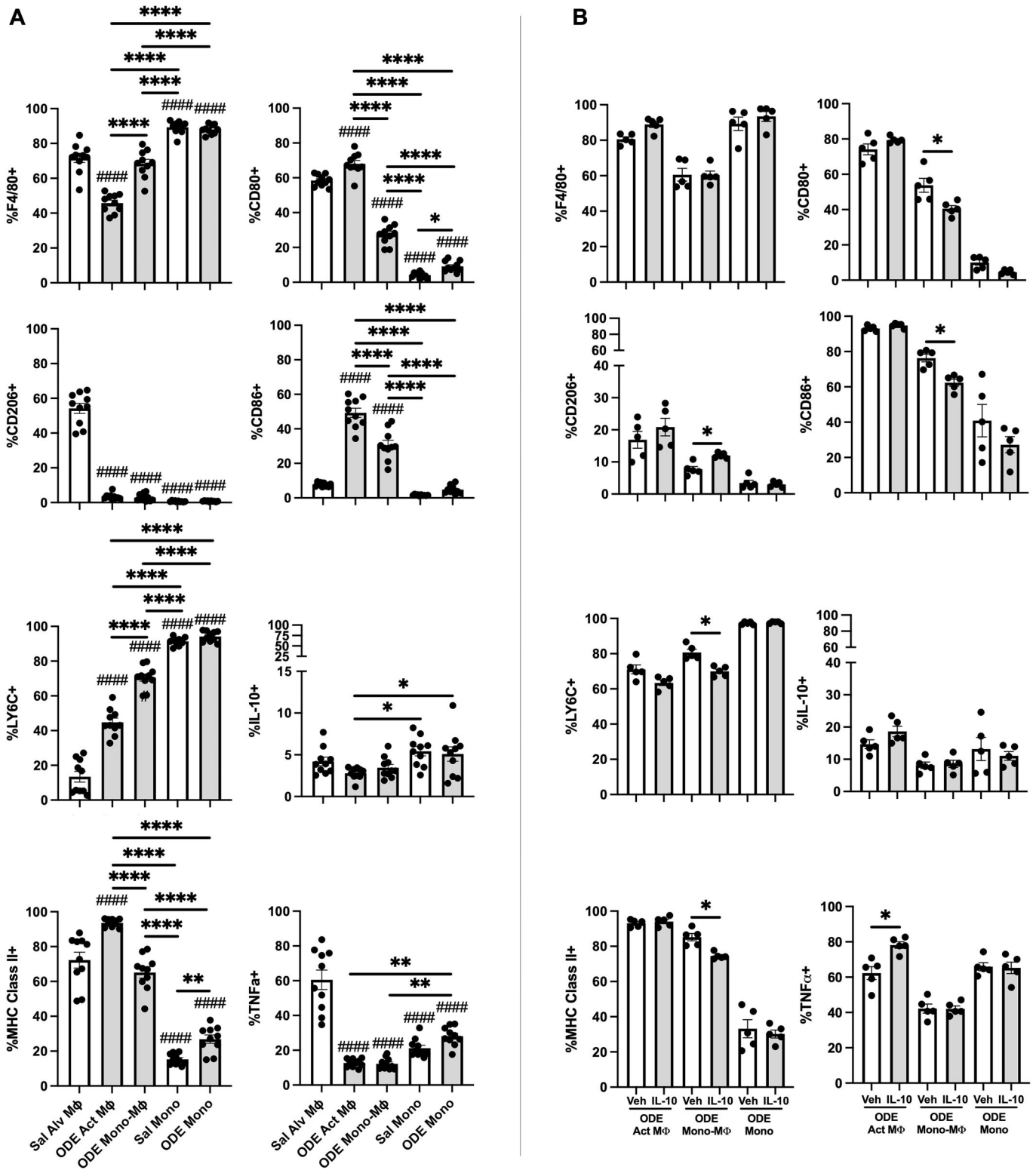


Figure 4. Lung-delivered IL-10 treatment following one-time 25% ODE exposure modulates immune phenotype of activated monocyte/macrophage Sub-populations. (A) Scatter-dot plots depict mean (\pm SEM bars) percent cell surface marker and intracellular cytokine (IL-10, TNF α) expression in monocyte/macrophage Sub-populations. $N = 10$ mice/group from two experimental runs. (B) Cell surface marker and intracellular cytokine percent expression of monocyte/macrophage Sub-populations exposed to ODE followed by treatment with vehicle (Veh) or IL-10. $N = 5$ mice/group from single experimental run. Statistical significance vs. Cxn (#### $p < 0.0001$); between groups (* $p < 0.05$, ** $p < 0.01$, *** $p < 0.0001$).

molecule) (Yang et al. 2022) expression was strikingly increased with ODE exposure in both ODE Act M Φ and ODE Mono-M Φ as compared to the Sal Alv M Φ , Sal Mono, and ODE Mono populations. A low proportion of cells across the monocyte/macrophage sub-populations exhibited intracellular IL-10 with both Sal and ODE Mono

populations expressing increased IL-10 expression vs. ODE Act M Φ . As compared to Sal Alv M Φ , intracellular TNF α expression was reduced in ODE Act M Φ , ODE Mono-M Φ , Sal Mono, and ODE Mono; however, intracellular TNF α expression was increased in ODE Mono vs. in ODE Act M Φ and ODE Mono-M Φ .

The effect of IL-10 treatment on ODE-modulated immunophenotype markers on Act M Φ , Mono-M Φ , and Mono was also assessed (Figure 4B). Notably, the recruited ODE Mono-M Φ sub-population was significantly modulated by IL-10 treatment—as marked by increased expression (vs. levels seen with vehicle) of anti-inflammatory CD206 and decreased expression of Ly6C, MHC Class II, and co-stimulatory molecules CD80 and CD86. Intracellular TNF α expression was increased in ODE Act M Φ treated with IL-10 vs. in vehicle control. There were no differences in intracellular IL-10 and cell surface F4/80 expression with IL-10 treatment vs. vehicle across the other monocyte-macrophage sub-populations.

ODE exposure induces functional changes in phagocytic ability and reactive oxygen species (ROS) production of lung monocyte/macrophage Sub-populations

Phagocytic activity (Figure 5A) and reactive oxygen species (ROS) production (Figure 5B) induced by 25% ODE exposure in the four monocyte-macrophage sub-populations was assessed. Results are depicted as percent positivity of the specific cell population of phagocytic or ROS index using mean fluorescence intensity (MFI) of the specific cell population relative to the mean MFI of Sal Alv M Φ to normalize across experiments. The data show that there was an increase in the percentage of cells phagocytosing the fluorescein-labeled *E. coli* BioParticles in the case of the ODE Act M Φ and ODE Mono-M Φ relative to that of the Sal Alv M Φ . Whereas there was no difference in percent BioParticle phagocytosis between ODE Mono vs. Sal Mono, the percent phagocytosis was decreased in ODE Mono vs. Sal Alv M Φ . Phagocytic activity of individual cells, quantified by phagocytic index (specific cell MFI divided by Sal Alv M Φ MFI), demonstrated increased phagocytic activity among the ODE Act M Φ , ODE Mono-M Φ , and Sal Mono vs. Sal Alv M Φ .

Monocyte/macrophage sub-populations exhibited ROS production (~100%). However, differences in ROS MFI were demonstrated with reduced ROS MFI index demonstrated with ODE Mono-M Φ , Sal Mono, and ODE Mono vs. Sal Alv M Φ . Similarly, the Sal and ODE Mono sub-populations exhibited decreased ROS vs. ODE Act M Φ . There were no differences in phagocytic activity or ROS production among all four monocyte/macrophage sub-populations with

IL-10 therapy relative to vehicle control following 25% ODE exposure (data not shown).

Lung-delivered IL-10 treatment reduces ODE-induced lung inflammation

Microscopic assessment of lung histopathology demonstrated that there was a reduction in ODE-induced bronchiolar and alveolar inflammation in mice that were treated with IL-10 as compared to what was seen with the vehicle controls (Figure 6). Using semi-quantitative assessment, lung inflammatory scores were shown to be increased by the ODE exposure at all concentrations (vs. control) and IL-10 therapy reduced inflammation for mice exposed to 12.5 or 25%, but not 50%, ODE.

Discussion

Occupational and environmental factors are a significant cause of debilitating lung diseases worldwide (Gorguner and Akgun 2010; Seaman et al. 2015). Novel therapeutic strategies are necessary for at-risk persons, and previous murine studies have demonstrated that short-term treatment with lung-delivered IL-10 reduced adverse lung effects induced by an acute LPS exposure (Poole et al. 2022). Here, preclinical animal studies demonstrated that short-term, lung-delivered IL-10 administration following various concentrations of a complex agriculturally-derived ODE exposure reduced ODE-induced systemic and lung inflammatory consequences. These beneficial effects with IL-10 therapy included blunting of ODE-induced weight loss, with corresponding reductions in ODE-induced acute phase protein pentraxin-2, airway pro-inflammatory cytokine/chemokine levels, neutrophil and recruited/transitioning CD11c^{int}CD11b⁺ monocyte-M Φ infiltrates, and lung pathology. The study also showed ODE exposure significantly modulated the immunophenotype and function of lung monocyte-M Φ sub-populations and that IL-10 then impacted this outcome. Specifically, IL-10 treatment increased anti-inflammatory CD206 expression and reduced pro-inflammatory (Ly6C) and antigen presentation (MHC Class II, CD80, CD86; M1-like) markers on the ODE-associated recruited/

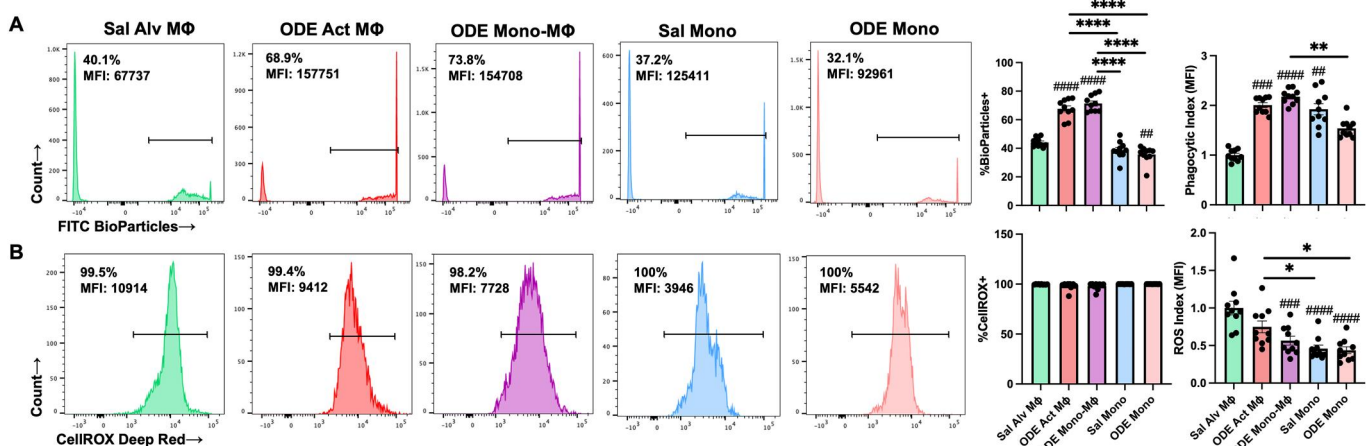


Figure 5. ODE exposure induces functional changes in lung monocyte/macrophage Sub-population phagocytic ability and reactive oxygen species (ROS) production. (A) Representative histograms depicting phagocytosed fluorescein-labeled *E. coli* BioParticles of saline (Sal) vs. ODE exposed monocyte-macrophage Sub-populations. Scatter-dot plots depict mean (\pm SEM) percent of cell Sub-population exhibiting BioParticle-specific fluorescence and the phagocytic index (mean fluorescence intensity (MFI) of positive BioParticle gate per Sub-population divided by MFI of Sal Alv M Φ positive BioParticle gate). (B) Representative histograms depicting ROS production determination by CellROX Deep Red fluorescence; scatter-dot plots depict percent of cell Sub-populations exhibiting CellROX Deep Red fluorescence and ROS index (MFI of positive CellROX gate per Sub-population divided by MFI of Sal Alv M Φ positive CellROX gate). $N = 10$ mice/group from two independent experiments. Statistical significance vs. Sal Alv M Φ denoted by ## $p < 0.01$, ### $p < 0.001$, #### $p < 0.0001$; between groups (* $p < 0.05$, ** $p < 0.01$, *** $p < 0.0001$).

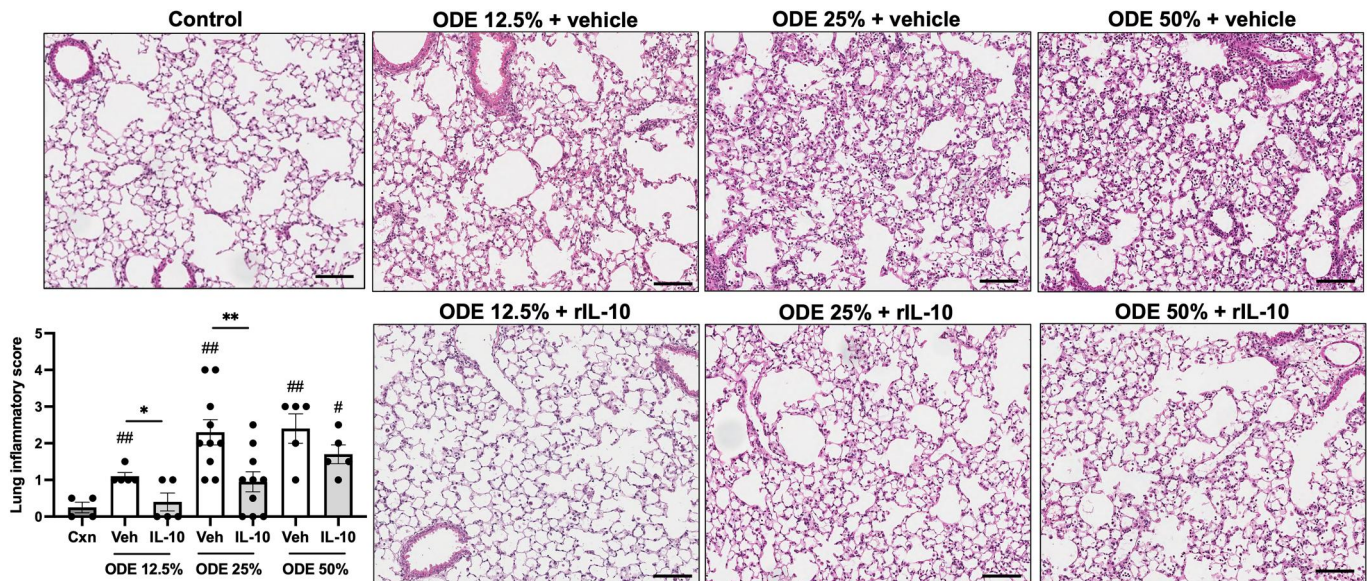


Figure 6. Treatment with IL-10 reduces ODE-induced lung inflammation. Representative H&E-stained lung section images from all treatment groups (ODE at various concentrations with IL-10 or saline vehicle treatment) and saline control. Scatter-dot plot depicts mean (\pm SEM) bars of semi-quantitative lung inflammatory scores per experimental treatment group. Individual values are averaged from 8 to 10 images/section/mouse. Statistical significance vs. Cxn ($^{\#}p < 0.05$, $^{\#\#}p < 0.01$); between groups ($^*p < 0.05$, $^{**}p < 0.01$). Line scale is 100 μ m.

transitioning $CD11c^{int}CD11b^{+}$ monocyte-M Φ sub-population. Collectively, these findings demonstrated the potential therapeutic benefit of short-term lung-delivered IL-10 in the context of an acute environmental and occupational exposure.

The focus of therapeutic approaches to treat environmental and occupational-associated diseases has centered on specific agent identification and risk reduction measures and mitigation (Schwab and Poole 2023). With a specificity for agriculture work settings, promotion of personal respiratory protection and exposure reduction measures are recommended. By using large animal (swine) confinement facility organic dust as a prototypical dust at escalating concentrations (i.e. 12.5, 25, 50%), our studies demonstrated clear dose-response systemic and airway inflammatory effects; these outcomes underscore the importance of ongoing efforts to reduce and prevent high-level exposures. However, the use of respiratory protection devices has been extremely low in agriculture work (<1%) (Davidson et al. 2018), though it was recently reported that 15.5% of young adult hog producers (age 18–30 years) state that they ‘always’ wear a N95 filtering facepiece respirator (Gibbs et al. 2023).

Moreover, it is also recognized that dust and endotoxin (surrogate of bacterial exposures) exposures in agriculture work are highly variable and often exceed occupational exposure limits by several orders of magnitude (Donham et al. 1995, 2000; Reynolds et al. 1996, 2013; Alvarado and Predicala 2019). For example, a recent study reported that a high proportion of United States dairy farm workers (89%) were exposed to inhalable endotoxin exceeding the occupational exposure limit with a geometric mean exposure of 438 EU/m³, 7-times the recommended average 54-hr workweek exposure (Davidson et al. 2018). Endotoxin concentrations in modern swine confinement facilities across the world have reported average levels up to 443 EU/m³ and 1260 EU/m³ of total dust (Roque et al. 2018). Thus, these current animal modeling concentrations would have relevance among animal production workers and furthermore highlight the unmet need to explore novel treatment strategies. Importantly, these current results show a striking beneficial effect of IL-10, even under these high experimental modeling conditions.

Lung monocytes-macrophages play a critical role in mediating responses to inflammatory bioaerosol exposure and recruited/transitional monocytes-macrophages are implicated in the transition of

acute inflammation to lung fibrosis in animal models and clinical investigations (Misharin et al. 2017; Verjans et al. 2018). Given the plasticity of lung monocytes/macrophages and their ability to elicit pro-resolving or injurious functions, these cells represent modifiable targets to mitigate tissue damage while hastening resolution. Here, lung-delivered IL-10 therapy profoundly reduced recruitment of the transitional $CD11c^{int}CD11b^{+}$ monocyte-M Φ in the case of all ODE test levels used, findings consistent with observations previously-reported following acute inhalant LPS exposure (Poole et al. 2022). This might be explained by IL-10 exerting an inhibitory effect on monocyte adhesion to endothelial cells, thus disabling monocyte recruitment to areas of inflammation (Mostafa Mtairag et al. 2001). In addition, IL-10 can block monocyte activation and proliferation, as well as prevent monocyte maturation and effector capabilities (Mu et al. 2005).

Lung monocyte-macrophage sub-populations are characteristically heterogeneous, with functional attributes that can be referred to as M1 (inflammatory) and M2 (anti-inflammatory, pro-fibrotic)-like macrophages (Azad et al. 2014). CD206 is a mannose receptor ubiquitously-expressed by normal human alveolar macrophages and recognized as a classic M2 marker (Bharat et al. 2016). Here, its exclusive expression was observed on control (saline) alveolar macrophages (Sal Alv M Φ) and its near-absent expression on ODE-associated Act M Φ and Mono-M Φ sub-populations. Such findings reflect a shift away from an M2-like macrophage. Whereas Ly6C expression is expressed on circulating monocytes, Ly6C up-regulation (as seen with ODE Act M Φ and ODE Mono-M Φ sub-populations) can also signify an activated macrophage state with inflammatory features (M1) (Yang et al. 2021). Interestingly, Ly6C^{hi} monocyte-macrophages have been characterized as pro-fibrotic in the liver (Ramachandran et al. 2012); in the lung, depletion of circulating Ly6C^{hi} monocytes reduces progression of bleomycin-induced pulmonary fibrosis (Gibbons et al. 2011). Future studies are warranted to target these transitioning Mono-M Φ with Ly6C^{hi} expression to fully understand their role in lung fibrosis.

Correspondingly, recruited ODE Mono-M Φ demonstrated increased antigen-presenting molecule (i.e. MHC Class II, CD80, CD86) expression as compared to lung monocytes, but expression of these molecules was not to the degree observed with the ODE Act

MΦ. The exact importance of this intermediate phenotype remains to be determined, but it appears to skew toward a M1 phenotype; moreover, these antigen-presenting molecules were down-regulated with IL-10 treatment in the CD11c^{int}CD11b⁺ Mono-MΦ. It should be noted that intracellular TNFα stores were reduced in ODE Act MΦ and ODE Mono-MΦ (vs. Sal Alv MΦ)—with corresponding increases in levels of extracellular TNFα airway levels—after ODE exposure. Moreover, IL-10 treatment increased intracellular TNFα stores in the ODE Act MΦ sub-population; this might be explained by IL-10 actions that inhibit release of pre-formed TNFα mediator stores (Armstrong et al. 1996). It is known that macrophage TNFα production and its downstream effects can be regulated by IL-10 as macrophage IL-10 activation inhibits the TNFα converting enzyme (ADAM-17) [through activation of TIMP3] to effectively shut down exposure-induced Toll-like receptor pathway activated TNFα release (Wyatt et al. 2020).

ODE exposure primed or enhanced phagocytic responses in the Act MΦ and Mono-MΦ sub-populations (vs. in Sal Alv MΦ). This finding extends *in vitro* observations that LPS (a component within ODE) increases the phagocytic ability (Islam et al. 2013) of lung-specific monocyte/macrophage sub-populations (Frevert et al. 1998). Here, IL-10 therapy did not alter or negatively affect ODE-mediated enhanced phagocytic ability, thus allowing for preservation of this important function used in host clearance of lung particulates/debris. All lung monocyte-macrophage sub-populations here exhibited normative ROS production, but the magnitude of this response (ROS index) was reduced in the more immature sub-populations (i.e. Mono-MΦ and monocytes). Correspondingly, there was no effect on ODE-dependent ROS production with IL-10 therapy.

In summary, the present findings support potential application of lung-delivered IL-10 therapy, particularly in the short-term, following an acute high-dose occupational/environmental inhalation exposure to organic dusts. Ultimately, such findings may go a long way to help reduce respiratory disease burdens in at-risk individuals.

Nevertheless, this study does have limitations. Whereas these studies may not reflect the exact human experiences in the field, the complexity intrinsic to the ODE is compositionally representative of real-world agriculture organic dust exposure. Future studies should also investigate effects of IL-10 therapy at potentially longer duration of use as well as in the setting of repeated occupational exposures and potentially as a prophylactic approach. It is noted that others have demonstrated that airway injury was reduced when human IL-10 expression was delivered by adenoviral vector treatment to the murine lung prior to LPS exposure (Garantziotis et al. 2006). Comprehensive assessment of the kinetics (e.g. deposition, lung cell uptake, degradation, and clearance) of IL-10 after administration in this setting is not known. Future studies should explore various approaches to enhance IL-10 drug delivery including novel nanoparticle formulations to maximize lung deposition and minimize pulmonary clearance of drugs for optimal lung-delivery strategies. Systemic IL-10 has been well-tolerated in human clinical interventions; however, anemia and thrombocytopenia have been reported with long-term use (Fioranelli and Grazia 2015). Thus, short term lung-delivery could potentially reduce untoward effects.

Acknowledgements

The authors acknowledge members of the Tissue Sciences Facility at the Department of Pathology and Microbiology (University of Nebraska Medical Center, Omaha, NE) for assistance with tissue processing and staining. We thank Victoria B. Smith, Holly Britton, and Craig Semerad in the Flow Cytometry Research Core Facility at

the University of Nebraska Medical Center for aid in flow cytometry studies. Schematics were created using www.BioRender.com.

Disclosure statement

Author J.A.P. received research reagent from AstraZeneca (no monies) and has been a site investigator for allergy and asthma clinical studies for Takeda, GlaxoSmithKline, Regeneron, and AstraZeneca (no monies). Authors A.D.S., R.G., A.J.N., A.G., D.J.R., T.A.W. do not declare any competing interests.

Funding

Funds for these studies were provided by National Institute for Occupational Safety and Health Grant U54OH010162 (ADS, TAW) and R01OH012045 (JAP), Department of Defense Grant #PR200793 (JAP). ADS, TAW, RG, and JAP received support from Central States Center of Agricultural Safety and Health (CS-CASH). TAW is supported by grants from the VA (BLR&D Merit I01 BX005886) and National Institutes of Health (P50 AA030407). TAW is the recipient of a Research Career Scientist Award (IK6 BX005962) from Department of Veterans Affairs. The UNMC Flow Cytometry Research Facility is administrated through the Office of the Vice Chancellor for Research and supported by state funds from the Nebraska Research Initiative (NRI) and The Fred and Pamela Buffett Cancer Center's National Cancer Institute Cancer Support Grant. Major instrumentation has been provided by the Office of the Vice Chancellor for Research, The University of Nebraska Foundation, the Nebraska Banker's Fund, and by the NIH-NCRR Shared Instrument Program.

References

- Agustí A, Edwards LD, Rennard SI, MacNee W, Tal-Singer R, Miller BE, Vestbo J, Lomas DA, Calverley PMA, Wouters E, et al. 2012. Evaluation of CLIPSEI – Persistent systemic inflammation is associated with poor clinical outcomes in COPD. A novel phenotype. *PLoS One*. 7(5):e37483. doi:10.1371/journal.pone.0037483.
- Alvarado A, Predicala B. 2019. Occupational exposure risk for swine workers in confined housing facilities. *J Agric Saf Health*. 25(1):37–50. doi:10.13031/jash.12990.
- American Thoracic Society. 1998. Official Conference Report of American Thoracic Society: Respiratory health hazards in agriculture. *Am J Respir Crit Care Med*. 158: S1–S76.
- Armstrong L, Jordan N, Millar A. 1996. Interleukin (IL)-10 regulation of tumor necrosis factor (TNF)-α from human alveolar macrophages and peripheral blood monocytes. *Thorax*. 51(2):143–149. doi:10.1136/thx.51.2.143.
- Azad A, Rajaram M, Schlesinger L. 2014. Exploitation of macrophage mannose receptor (CD206) in infectious disease diagnostics and therapeutics. *J Cytol Mol Biol*. 1(1):1000003. doi:10.13188/2325-4653.1000003.
- Basinas I, Sigsgaard T, Kromhout H, Heederik D, Wouters IM, Schläpfer V. 2015. A comprehensive review of levels and determinants of personal exposure to dust and endotoxin in livestock farming. *J Expo Sci Environ Epidemiol*. 25(2):123–137. doi:10.1038/jes.2013.83.
- Bharat A, Borade SM, Morales-Nebreda L, McQuattie-Pimentel AC, Soberanes S, Ridge K, DeCamp MM, Mestan KK, Perlman H, Budinger GRS, et al. 2016. Flow cytometry reveals similarities between lung macrophages in humans and mice. *Am J Respir Cell Mol Biol*. 54(1):147–149. doi:10.1165/rcmb.2015-0147LE.
- Boissy R, Romberger D, Roughead W, Weissenburger-Moser L, Poole J, LeVan T. 2014. Shotgun pyrosequencing metagenomic analyses of dusts from swine confinement and grain facilities. *PLoS One*. 9(4):e95578. doi:10.1371/journal.pone.0095578.
- Davidson M, Schaeffer J, Clark M, Magzamen S, Brooks E, Keefe T, Bradford M, Roman-Muniz N, Mehaffy J, Dooley G, et al. 2018. Personal exposure of dairy workers to dust, endotoxin, muramic acid, ergosterol, and ammonia on large-scale dairies in the high plains Western United States. *J Occup Environ Hyg*. 15(3):182–193. doi:10.1080/15459624.2017.1403610.

- Donham K, Cumro D, Reynolds S, Merchant J. 2000. Dose-response relationships between occupational aerosol exposures and cross-shift declines of lung function in poultry workers: Recommendations for exposure limits. *J Occup Environ Med.* 42(3):260–269. doi:10.1097/00043764-200003000-00006.
- Donham K, Reynolds S, Whitten P, Merchant J, Burmeister L, Popendorf W. 1995. Respiratory dysfunction in swine production facility workers: Dose-response relationships of environmental exposures and pulmonary function. *Am J Ind Med.* 27(3):405–418. doi:10.1002/ajim.4700270309.
- Fioranelli M, Grazia R. 2015. Twenty-five years of studies and trials for the therapeutic application of IL-10 immunomodulating properties. From high doses administration to low dose medicine new paradigm. *J Integr Cardiol.* 1:2–6.
- Frevert C, Warner A, Weller E, Brain J. 1998. The effect of endotoxin on *in vivo* rat alveolar macrophage phagocytosis. *Exp Lung Res.* 24(6):745–758. doi:10.3109/0190214980909593.
- Garantzotis S, Brass DM, Savov J, Hollingsworth JW, McElvania-TeKippe E, Berman K, Walker JK, Schwartz DA. 2006. Leukocyte-derived IL-10 reduces subepithelial fibrosis associated with chronically inhaled endotoxin. *Am J Respir Cell Mol Biol.* 35(6):662–667. doi:10.1165/rcmb.2006-0055OC.
- Gibbons M, MacKinnon A, Ramachandran P, Dhaliwal K, Duffin R, Phythian-Adams A, van Rooijen N, Haslett C, Howie S, Simpson A, et al. 2011. Ly6C^{hi} monocytes direct alternatively-activated pro-fibrotic macrophage regulation of lung fibrosis. *Am J Respir Crit Care Med.* 184(5):569–581. doi:10.1164/rccm.201010-1719OC.
- Gibbs J, Sheridan C, Sullivan D, Rautiainen R, Nonnenmann M, Wyatt T. 2023. Self-reported respiratory health symptoms and respiratory protection behaviors of young adult hog producers in the United States. *Am J Ind Med.* 66(9):794–804. doi:10.1002/ajim.23515.
- Gorguner M, Akgun M. 2010. Acute inhalation injury. *Eurasian J Med.* 42(1):28–35. doi:10.5152/eajm.2010.09.
- Hu G, Christman J. 2019. Alveolar macrophages in lung inflammation and resolution. *Front Immunol.* 10:2275. doi:10.3389/fimmu.2019.02275.
- Islam MA, Pröll M, Hölker M, Tholen E, Tesfaye D, Looft C, Schellander K, Cinar MU. 2013. Alveolar macrophage phagocytic activity is enhanced with LPS priming, and combined stimulation of LPS and lipoteichoic acid synergistically induce pro-inflammatory cytokines in pigs. *Innate Immun.* 19(6):631–643. doi:10.1177/1753425913477166.
- LeVan T, Romberger D, Siahpush M, Grimm B, Ramos A, Johansson P, Michaud T, Heires A, Wyatt T, Poole J. 2018. Relationship of systemic IL-10 levels with pro-inflammatory cytokine responsiveness and lung function in agriculture workers. *Respir Res.* 19(1):166. doi:10.1186/s12931-018-0875-z.
- Madsen A, Tendal K, Schlunssen V, Heltberg I. 2012. Organic dust toxic syndrome at a grass seed plant caused by exposure to high concentrations of bioaerosols. *Ann Occup Hyg.* 56:776–788.
- May S, Romberger D, Poole J. 2012. Respiratory health effects of large animal farming environments. *J Toxicol Environ Health B Crit Rev.* 15(8):524–541. doi:10.1080/10937404.2012.744288.
- Mikuls TR, Gaurav R, Thiele GM, England BR, Wolfe MG, Shaw BP, Bailey KL, Wyatt TA, Nelson AJ, Duryee MJ, et al. 2021. Impact of airborne endotoxin exposure on rheumatoid arthritis-related joint damage, autoantigen expression, autoimmunity, and lung disease. *Int Immunopharmacol.* 100:108069. doi:10.1016/j.intimp.2021.108069.
- Misharin AV, Morales-Nebreda L, Reyfman PA, Cuda CM, Walter JM, McQuattie-Pimentel AC, Chen C-I, Anekalla KR, Joshi N, Williams KJN, et al. 2017. Monocyte-derived alveolar macrophages drive lung fibrosis and persist in the lung over the life span. *J Exp Med.* 214(8):2387–2404. doi:10.1084/jem.20162152.
- Mostafa Mtaïrag E, Chollet-Martin S, Oudghiri M, Laquay N, Jacob M, Michel J, Feldman L. 2001. Effects of IL-10 on monocyte/endothelial cell adhesion and MMP-9/TIMP-1 secretion. *Cardiovasc Res.* 49(4):882–890. doi:10.1016/s0008-6363(00)00287-x.
- Mu W, Ouyang X, Agarwal A, Zhang L, Long DA, Cruz PE, Roncal CA, Glushakova OY, Chiodo VA, Atkinson MA, et al. 2005. IL-10 suppresses chemokines, inflammation, and fibrosis in a model of chronic renal disease. *J Am Soc Nephrol.* 16(12):3651–3660. doi:10.1681/ASN.2005030297.
- Nelson A, Roy S, Warren K, Janike K, Thiele G, Mikuls T, Romberger D, Wang D, Swanson B, Poole J. 2018. Sex differences impact the lung-bone inflammatory response to repetitive inhaled lipopolysaccharide exposures in mice. *J Immunotoxicol.* 15(1):73–81. doi:10.1080/1547691X.2018.1460425.
- Nordgren T, Bailey K. 2016. Pulmonary health effects of agriculture. *Curr Opin Pulm Med.* 22(2):144–149. doi:10.1097/MCP.0000000000000247.
- Park Y, Ahn C, Kim T. 2021. Occupational and environmental risk factors of idiopathic pulmonary fibrosis: A systematic review and meta-analyses. *Sci Rep.* 11(1):4318. doi:10.1038/s41598-021-81591-z.
- Poole J, Gaurav R, Schwab A, Nelson A, Gleason A, Romberger D, Wyatt T. 2022. Post-endotoxin exposure-induced lung inflammation and resolution consequences beneficially impacted by lung-delivered IL-10 therapy. *Sci Rep.* 12(1):17338. doi:10.1038/s41598-022-22346-2.
- Poole J, Gleason A, Bauer C, West W, Alexis N, Reynolds S, Romberger D, Kielian T. 2012. T-cells and a mixed T_{H1}/T_{H17} response are important in organic dust-induced airway disease. *Ann Allergy Asthma Immunol.* 109(4):266–273.e2. doi:10.1016/j.anaai.2012.06.015.
- Poole J, Mikuls T, Duryee M, Warren K, Wyatt T, Nelson A, Romberger D, West W, Thiele G. 2017. A role for B-cells in organic dust induced lung inflammation. *Respir Res.* 18(1):214. doi:10.1186/s12931-017-0703-x.
- Poole J, Thiele G, Janike K, Nelson A, Duryee M, Rentfro K, England B, Romberger D, Carrington J, Wang D, et al. 2019. Combined collagen-induced arthritis and organic dust-induced airway inflammation to model inflammatory lung disease in rheumatoid arthritis. *J Bone Miner Res.* 34(9):1733–1743. doi:10.1002/jbmr.3745.
- Poole J, Wyatt T, Oldenburg P, Elliott M, West W, Sisson J, von Essen S, Romberger D. 2009. Intranasal organic dust exposure-induced airway adaptation response marked by persistent lung inflammation and pathology in mice. *Am J Physiol Lung Cell Mol Physiol.* 296(6):L1085–1095. doi:10.1152/ajplung.90622.2008.
- Poole J. 2012. Farming-associated environmental exposures and effect on atopic diseases. *Ann Allergy Asthma Immunol.* 109(2):93–98. doi:10.1016/j.anaai.2011.12.014.
- Ramachandran P, Pellicoro A, Vernon M, Boulter L, Aucott R, Ali A, Hartland S, Snowdon V, Cappon A, Gordon-Walker T, et al. 2012. Differential Ly6C expression identifies the recruited macrophage phenotype, which orchestrates the regression of murine liver fibrosis. *Proc Natl Acad Sci USA.* 109(46):E3186–3195. doi:10.1073/pnas.1119964109.
- Reynolds S, Donham K, Whitten P, Merchant J, Burmeister L, Popendorf W. 1996. Longitudinal evaluation of dose-response relationships for environmental exposures and pulmonary function in swine production workers. *American J Industrial Med.* 29(1):33–40. doi:10.1002/(SICI)1097-0274(199601)29:1<33::AID-AJIM5>3.0.CO;2-#.
- Reynolds S, Nonnenmann M, Basinas I, Davidson M, Elfman L, Gordon J, Kirychuck S, Reed S, Schaeffer J, Schenker M, et al. 2013. Systematic review of respiratory health among dairy workers. *J Agromedicine.* 18(3):219–243. doi:10.1080/1059924X.2013.797374.
- Robbe P, Draijer C, Borg T, Luinge M, Timens W, Wouters I, Melgert B, Hylkema M. 2015. Distinct macrophage phenotypes in allergic and non-allergic lung inflammation. *Am J Physiol Lung Cell Mol Physiol.* 308(4):L358–367. doi:10.1152/ajplung.00341.2014.
- Roche P, Furuta K. 2015. The ins and outs of MHC Class II-mediated antigen processing and presentation. *Nat Rev Immunol.* 15(4):203–216. doi:10.1038/nri3818.
- Roque K, Shin K, Jo J, Lim G, Song E, Shin S, Gautam R, Lee J, Kim Y, Cho A, et al. 2018. Association between endotoxin levels in dust from indoor swine housing environments and the immune responses of pigs. *J Vet Sci.* 19(3):331–338. doi:10.4142/jvs.2018.19.3.331.
- Roszer T. 2015. Understanding the mysterious M2 macrophage through activation markers and effector mechanisms. *Mediators Inflamm.* 2015:816460.
- Schwab A, Poole J. 2023. Mechanistic and therapeutic approaches to occupational exposure-associated allergic and non-allergic asthmatic disease. *Curr Allergy Asthma Rep.* 23(6):313–324. doi:10.1007/s11882-023-01079-w.
- Seaman D, Meyer C, Kanne J. 2015. Occupational and environmental lung disease. *Clin Chest Med.* 36(2):249–268. doi:10.1016/j.ccm.2015.02.008.
- Sigsgaard T, Basinas I, Doeke G, de Blay F, Folletti I, Heederik D, Lipinska-Ojrzanowska A, Nowak D, Olivieri M, Quirce S, et al. 2020. Respiratory diseases and allergy in farmers working with livestock: An EAACI position paper. *Clin Transl Allergy.* 10(1):29. doi:10.1186/s13601-020-00334-x.
- Verjans E, Kanzler S, Ohl K, Rieg A, Ruske N, Schippers A, Wagner N, Tenbroek K, Uhlig S, Martin C. 2018. Initiation of LPS-induced pulmonary dysfunction and its recovery occur independent of T-cells. *BMC Pulm Med.* 18(1):174. doi:10.1186/s12890-018-0741-2.
- Wang X, Zhao W, Ransohoff R, Zhou L. 2018. Infiltrating macrophages are broadly activated at the early stage to support acute skeletal muscle injury repair. *J Neuroimmunol.* 317:55–66. doi:10.1016/j.jneuroim.2018.01.004.
- Warren K, Wyatt T, Romberger D, Ailts I, West W, Nelson A, Nordgren T, Staab E, Heires A, Poole J. 2017. Post-injury and resolution response to repetitive inhalation exposure to agricultural organic dust in mice. *Safety.* 3(1):3. doi:10.3390/safety3010010.

- Wunschel J, Poole J. 2016. Occupational agriculture organic dust exposure and its relationship to asthma and airway inflammation in adults. *J Asthma*. 53(5):471–477. doi:10.3109/02770903.2015.1116089.
- Wyatt T, Nemecek M, Chandra D, DeVasure J, Nelson A, Romberger D, Poole J. 2020. Organic dust-induced lung injury and repair: Bi-directional regulation by TNF α and IL-10. *J Immunotoxicol*. 17(1):153–162. doi:10.1080/1547691X.2020.1776428.
- Yang M, Tian S, Lin Z, Fu Z, Li C. 2022. Co-stimulatory and co-inhibitory molecules of B7-CD28 family in cardiovascular atherosclerosis: A review. *Medicine*. 101(45):e31667. doi:10.1097/MD.00000000000031667.
- Yang P, Liu L, Sun L, Fang P, Snyder N, Saredy J, Ji Y, Shen W, Qin X, Wu Q, et al. 2021. Immunological feature and transcriptional signaling of Ly6C monocyte subsets from transcriptome analysis in control and hyper-homocysteinemic mice. *Front Immunol*. 12:632333. doi:10.3389/fimmu.2021.632333.